Journal of Radioanalytical and Nuclear Chemistry (2024) 333:3487–3496
https://doi.org/10.1007/s10967-023-09290-9

An extended Monte Carlo simulation code for modeling gas chromatography experiments with superheavy elements and their homologs

Dominik Dietzel[1,2] · **Alexander Yakushev**[2] · **Christoph E. Düllmann**[1,2,3]

Received: 25 September 2023 / Accepted: 21 November 2023 / Published online: 28 May 2024

Abstract
Monte Carlo simulations are commonly used to model the behavior of chemical species of the heaviest elements and their homologs in gas chromatography experiments. In this paper, we present an extension of the fundamental Monte Carlo simulation proposed by Zvara in 1985. While preserving the core functionality, our code features two enhancements: first, it allows simulating experiments in which a primary radioisotope decays into a daughter isotope belonging to a different element, hence exhibiting different chemical properties. Second, it allows modeling scenarios where conversion of an initial chemical species to a different one can occur at temperatures high enough to overcome an activation barrier, facilitating simulations of related physisorption and chemisorption processes. This Monte Carlo code is applicable to open tubular and rectangular chromatography columns.

Keywords Monte Carlo simulation · Gas chromatography · Superheavy elements · Precursor effect · Activation energy barrier

Introduction

The synthesis and characterization of SuperHeavy Elements (SHE) represent an intriguing interdisciplinary field, but they also present unique challenges for both physicists and chemists [1, 2]. Gas phase chemical methods have proven powerful for the investigation of the heaviest known elements [3]. Small production rates and short half-lives lead to such experiments being performed with single-atom-at-a-time quantities [4, 5]. The two most widely used techniques are isothermal gas chromatography (IC) and thermochromatography (TC). In IC, several experiments are conducted with the chromatography column kept at an isothermal temperature and the fraction an ensemble of radioactive atoms surviving passage through the column is measured. This fraction decreases with decreasing temperature due to the increase of the residence time spent in the adsorbed state, leading to increasing losses due to radioactive decay of the studied radioisotope inside the column. For reference, examples of IC experiments involving molecules of SHE like SgO_2Cl_2, $SgO_2(OH)_2$, $DbOCl_3$ and BhO_3Cl can be found in [6–9]. In the past, chemical studies were performed using IC setups like OLGA [10, 11] and IVO [12]. A disadvantage of the classical IC method is the need to perform experiments at low temperatures, where SHE are not detected as they decay inside the chromatography column, which is unfavorable in light of the low production rate of SHE. To detect the decay of elements inside the column during the experiment, first the CTS (Cryo-Thermochromatography Setup) [13] and following shortly after the COLD (Cryo On-Line Detector) detection and chromatography setup were developed, which consist of a chromatography channel formed by PIN-diode detectors facing each other [14]. Further developments include the COMPACT (Cryo-Online Multidetector for Physics and Chemistry of Transactinides) [15, 16] and most recently the miniCOMPACT [17] setups. Such setups can also be cooled to low temperatures, to capture and detect

✉ Dominik Dietzel
dietzel@uni-mainz.de

[1] Department of Chemistry – TRIGA Site, Johannes Gutenberg-Universität Mainz, Fritz-Strassmann-Weg 2, 55128 Mainz, Germany

[2] GSI Helmholtzzentrum Für Schwerionenforschung GmbH, Planckstraße 1, 64291 Darmstadt, Germany

[3] Helmholtz-Institut Mainz, Staudingerweg 18, 55128 Mainz, Germany

even volatile species like HsO_4 [14], copernicium [18, 19] and flerovium [15, 20].

The second approach, called thermochromatography (TC), in which a negative temperature gradient is applied along the column, covers a bigger temperature range, usually starting from around 1000 °C. The carrier gas transports the species under study to ever lower temperatures, until radioactive decay sets in faster than further transport does. Scanning the chromatography column (in case of passive columns) or registration inside columns made of nuclear detectors like COLD or COMPACT yields a deposition peak of the studied chemical species at a temperature that is characteristic for the interaction strength of the species with the column surface material [3].

Results obtained with single-atom quantities of the heaviest elements are compared to results obtained with tracer amounts of short-lived isotopes of the lighter homologs. This comparison provides a more direct link to classical chemical data obtained with macroscopic amounts.

Chemical properties of superheavy elements and their homologs are investigated under similar experimental conditions, at a single-atom level. Unlike in experiments with macroscopic amounts, the concentration distribution between two phases in the separation process cannot be determined due to low production rates. Therefore, in the law of mass action in a chemical equilibrium, concentrations of the species are replaced with the number of atoms in both phases [21]. In gas-phase experiments, single atoms traverse two phases: the mobile gaseous and the stationary solid phase, where the species of interest temporarily immobilize on a surface through adsorption. Therefore, the interaction strength of the element with a surface is a fundamental property that is quantified using the adsorption enthalpy (ΔH_{ads}). As the atom is adsorbed onto the stationary phase for a period of time dependent on the interaction strength, it can be desorbed back into the mobile phase. The assumption here is that the desorption energy is equal in magnitude but opposite in sign to the adsorption enthalpy. In chromatography columns, the adsorption and desorption processes are repeated many times to improve separation between the species. Different approaches have been described in the literature to obtain quantitative data, e.g., ΔH_{ads} (typically given in kJ/mol) of the atom or compound on the column material. In single atom gas chromatography experiments, macroscopic parameters as such can be obtained from the deposition temperature and retention time using either the second law or the quasi third law method as described in [22].

In 1985, I. Zvara proposed the use of Monte-Carlo-simulations (MCS) as an alternative method to derive values of the adsorption enthalpy on heterosurfaces from experimental data [23]. This approach has gained increasing attention and is now widely used in the field of SHE chemistry. Such simulations complement gas–solid chromatography experiments of atoms and compounds of SHE and their lighter homologs, aiming to determine thermodynamic values [1, 3, 24, 25]. In the MCS-based analysis of experiments with single atoms (or molecules) of SHE and their homologs, the adsorption enthalpy of one or multiple species can be determined by comparing the results of these experiments to Monte Carlo simulation with parameters similar to the experiments. The detailed approach of the simulation is already described in [23, 26]. This code has been adapted to various setups and experiments already, for example to the rectangular channel of the COMPACT or miniCOMPACT detector [27].

The MCS simulates the migration of a single atom or molecule through the chromatography column, using actual experimental parameters like dimension of the column, gas type and flow rate, nuclide half-life etc. For the simulation of the individual history of one atom, the simulation uses random quantities derived from exponential probability distributions with a mean value for the lifetime t_f of the atom, the length and duration of long jumps η_j and t_{η_j} between two encounters with the surface and the deposition time from sequential surface encounters τ_{Ns}. Each parameter follows its own probability distribution. All N atoms (i = 1 to N) in the column start at $x_i = 0$, the beginning of the column. A random jump length $\eta_{j,i}$ is calculated for each atom based on the mean jump length η_j, which considers the current temperature of the column T(x) at position x_i. The jump length is added to the current position. These "long jumps" neglect the microscopic displacements: "Once the molecule encounters the surface, it, as a rule, experiences a series of adsorption–desorption events proceeding without a change in the x coordinate. These sequences are intermittent with rather long downstream jumps, η, …" [23]. After the jump, a random residence time is calculated using the mean time of adsorption (Eq. 1), multiplied by the number of surface encounters in the first series of only small displacements at the surface before the next long downstream jump. The summed time of adsorption gets added to the total time, which is then compared to the lifetime of the species. If the accumulated time exceeds the atom's lifetime, the last position is recorded as the position where decay occurred and is stored in an array that stores the distribution of decay positions from all atoms. This procedure yields an individual decay position of the radioactive atom or molecule. Repeating this simulation for many atoms (typically 10.000 to 1.000.000) yields simulated distributions of the activity for a IC or TC experiment or breakthrough curves for a series of IC experiments for a given value of $\Delta H_{ads.}$. The value used in the simulation that best matches the experimental result is then taken as the experimental result, and its uncertainties are often evaluated as well.

A simple model of adsorption, known as reversible mobile adsorption, suggests that species exhibit high retention at low temperatures and low retention at high temperatures. This process is fully reversible, and thus, $\Delta H_{ads.}$ equals the desorption enthalpy $\Delta H_{des.}$ [22, 26]. The adsorbed species is allowed to vibrate perpendicular to the surface, with the frequency of the surface. The residence time of a species on the surface is calculated using Frenkel's Eq. (1).

$$\overline{\tau}_a = \tau_0 \exp(-\Delta H_{ads}/RT) \quad (1)$$

Equation (1) shows the formula for the mean adsorption time $\overline{\tau}_a$. τ_0 is the period of oscillation of the atom perpendicular to the surface, $\Delta H_{ads.}$ is the adsorption enthalpy in kJ/mol, R the gas constant and T the temperature in K.

Mobile adsorption can be used to describe the migration process when a species does not undergo a chemical reaction. For instance, this is applicable in experiments with inert surfaces like cold SiO_2 and non-reactive species. Since this is only the case in some species, this calls for a modification and extension of the basic model of the mobile adsorption in the MCS. In this work, we present extensions to the well-proven MCS approach to evaluate chemical properties of SHE and their lighter homologs obtained in IC and in TC experiments. Our extended codes explicitly include the proper treatment of the two following cases:

(i) On the chemistry side, it accounts for the possibility of chemical reactions with the surface to another species with different properties, extending the mobile adsorption process by incorporating a more detailed and accurate model of surface interaction (Chemical reactions superimposing the mobile adsorption process)
(ii) On the nuclear side, it allows the simulation of two species connected through the decay of the initial mother nuclide (precursor effect and implantation probability).

Chemical reactions superimposing the mobile adsorption process

Although the analysis of experiments with superheavy elements and their lighter homologs using a MCS based on the process of mobile adsorption and is well established, not all experimental results can be described by simulations using only this simple adsorption–desorption process. Since the residence time at the surface and therefore the distribution in the column is only dependent on the adsorption/desorption enthalpy, the process of mobile adsorption does not always correspond to reality. A simulation based solely on one value for $\Delta H_{ads.}$ does not account, e.g., for the presence of different binding sites on the inhomogeneous surface, diffusion on the surface to stronger binding sites [20] or diffusion in the surface. Furthermore, it neglects chemical processes like reactions with the surface, aerosols or filters. Especially at high temperatures, such reactions can lead to the formation of strong bonds (chemisorption) and alter the species chemically. Consequently, reaction products may exhibit different adsorption enthalpies compared to the original species. In certain regions of the column with elevated temperatures, species can react with the surface (e.g., with an oxygen atom of the quartz surface), resulting in the formation of compounds that may be more volatile or less compared to the original species, that deposits at a different temperature. An example of a chemical transport reaction can be found in [6]. In experiments with possibly reactive surfaces, the possibility of a chemical reaction is disregarded or not discussed [28]. On the other hand, multiple gas-phase reactions have been investigated in experiments using a mixture of chlorinating and oxygenating gases [6, 9, 29] or CO as a reactive gas [30].

To further evaluate and describe the complex interaction mechanisms at the surface of the column, an activation energy barrier has been implemented into the MCS, which allows for the independent coupled simulation of (i) adsorption of a primary species, (ii) possible chemical reaction at the surface, and (iii) desorption of non-reacted species or the surface reaction product.

In this approach, the nucleus of the atom remains unchanged, while the species undergoes chemical reaction. When an atom approaches the surface, it can initially be held by the dispersive force, resulting in a physisorbed state. From this state, the atom may either desorb back into the gas phase or form a stronger bond (chemisorbed state) with the surface [31]. The transition from the physisorbed to the chemisorbed state can occur with or without an activation barrie (Fig. 1). The simulation incorporating the activation energy barrier and surface chemical reactions requires additional parameters to describe the more intricate surface interaction process. These parameters include:

1. $\Delta H_{ads,1}$: Adsorption enthalpy by the first-chance adsorption of the species from the gas phase to the surface due to physical adsorption without formation of a chemical bond.
2. E_a: The activation energy determines if an atom can form a stronger bond with the surface and engage in an irreversible reaction with a second species having distinct properties. The likelihood of surpassing the activation energy barrier relies on its magnitude, the current temperature, and the duration of adsorption on the surface, which is calculated using $\Delta H_{ads,1}$. An atom in the gas stream cannot interact with the surface and therefore not attempt to pass the energy barrier.

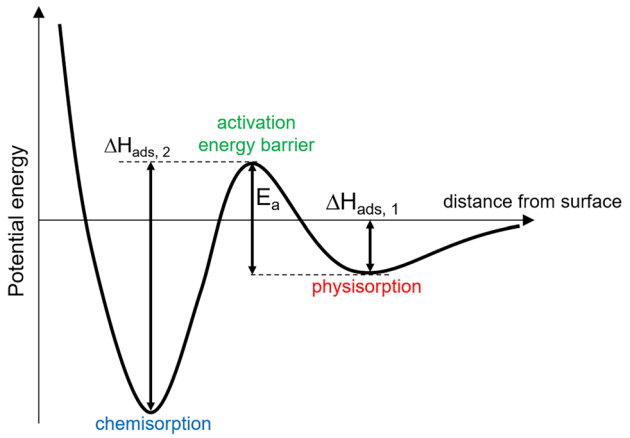

Fig. 1 Schematic one-dimensional diagram of the potential energy of an atom near the surface. After physisorption, the activation energy barrier could be passed under certain circumstances, leading to the strongly bound non-reversible chemisorption state (after [32])

3. $\Delta H_{ads,2}$: This parameter represents the adsorption enthalpy after surpassing the activation energy barrier. It characterizes the interaction strength between the species and the surface upon barrier crossing. It could be seen as the adsorption enthalpy of a second species (for example a hydride, hydroxide or oxide), resulting from the reaction (chemical bond formation) or binding to a more energetically favorable site due to surface diffusion. This enthalpy could significantly deviate from $\Delta H_{ads,1}$.

In cases where the activation barrier is negligible, $\Delta H_{ads.}$ of the chemisorbed species can be directly used to calculate the residence time. In such situations, no modification of the mobile adsorption mechanism is necessary for the Monte Carlo simulation. However, if the activation barrier is higher than the energy required for desorption from the physisorbed state, the probability of barrier penetration needs to be introduced into the simulation. The probability of passing the barrier is calculated for a number of vibrational attempts during the residence time τ_a and for the activation energy value E_a. The number of attempts required to surpass the activation barrier, and consequently the time needed, depends on the height of the barrier. A longer immobilization on the surface, resulting from stronger adsorption enthalpy values, increases the likelihood of successfully overcoming the activation barrier. This can lead to even stronger adsorption or the formation of chemical bonds between the atom and the surface. The formula for the probability of the atom of passing the activation energy barrier is given in Eq. (2). It contains the activation energy E_a and the physisorption time on the surface $\tau_{a,i}$.

$$P \propto 1 - \left(1 - e^{-E_a/RT}\right)^{\tau_{a,i}/\tau_0} \quad (2)$$

Equation (2) summarizes all attempts of the atom to pass the barrier in the time it spends in the adsorbed state. $\tau_{a,i}/\tau_0$ is the number of attempts to pass the barrier, calculated by the adsorption time $\tau_{a,i}$ divided by the vibrational period τ_0. The term $\exp(-E_a/RT)$ expresses the probability of passing the barrier in a single attempt and is derived from the number of atoms/molecules above the energy E_a in the Boltzmann distribution. A random function (0–1) is utilized to test if $1\text{-}random() < P$. If the condition is fulfilled and the activation energy barrier is surpassed, a new residence time is calculated for the stronger interaction (chemisorption) with a different ΔH_{ads}. After being adsorbed on the surface, the species has the potential to desorb and resume its travel along the column. This desorption can occur either as the same species if the formed chemical bond(s) is (are) broken, or as a different species altogether. In the latter case, different properties, including the diffusion coefficient and the adsorption enthalpy are assigned to the traveling species. Figure 2a shows a simplified flow scheme of the simulation.

Precursor effect and implantation probability

Similar to chemical reactions, the nuclear decay of an atom during the experiment can change its properties significantly. Some of the superheavy elements and also some of the lighter homologs are not produced directly, but through a precursor, which alpha decays to the desired element. At first, this element is ionized, but gets neutralized in the environment eventually. If the precursor itself lives long enough for diffusion towards the surface, chemical interaction with the surface or transport in the column, it can significantly influence the distribution of its daughter.

The precursor effect accounts for the formation of new species through radioactive decay, with the precursor having already interacted with the solid phase and established a distribution in the chromatography column. The simulation including the precursor effect is particularly relevant for experiments where the investigated species is not directly produced. The precursor's impact grows with longer lifetime and higher reactivity of the mother atom. In homolog studies with elements that can only be produced via a precursor, the advanced simulation can be employed to determine $\Delta H_{ads.}$ of the daughter species or provide an estimate for the limit for diffusion-controlled adsorption, given the known properties of the mother atom. For instance, we consider the system ^{211}Pb/^{211}Bi ($t_{1/2}$ = 36.1 min / 2.14 min), where the precursor lead is long-lived and non-volatile at ambient temperature on the quartz surface [33]. The system ^{288}Mc/^{284}Nh is an example

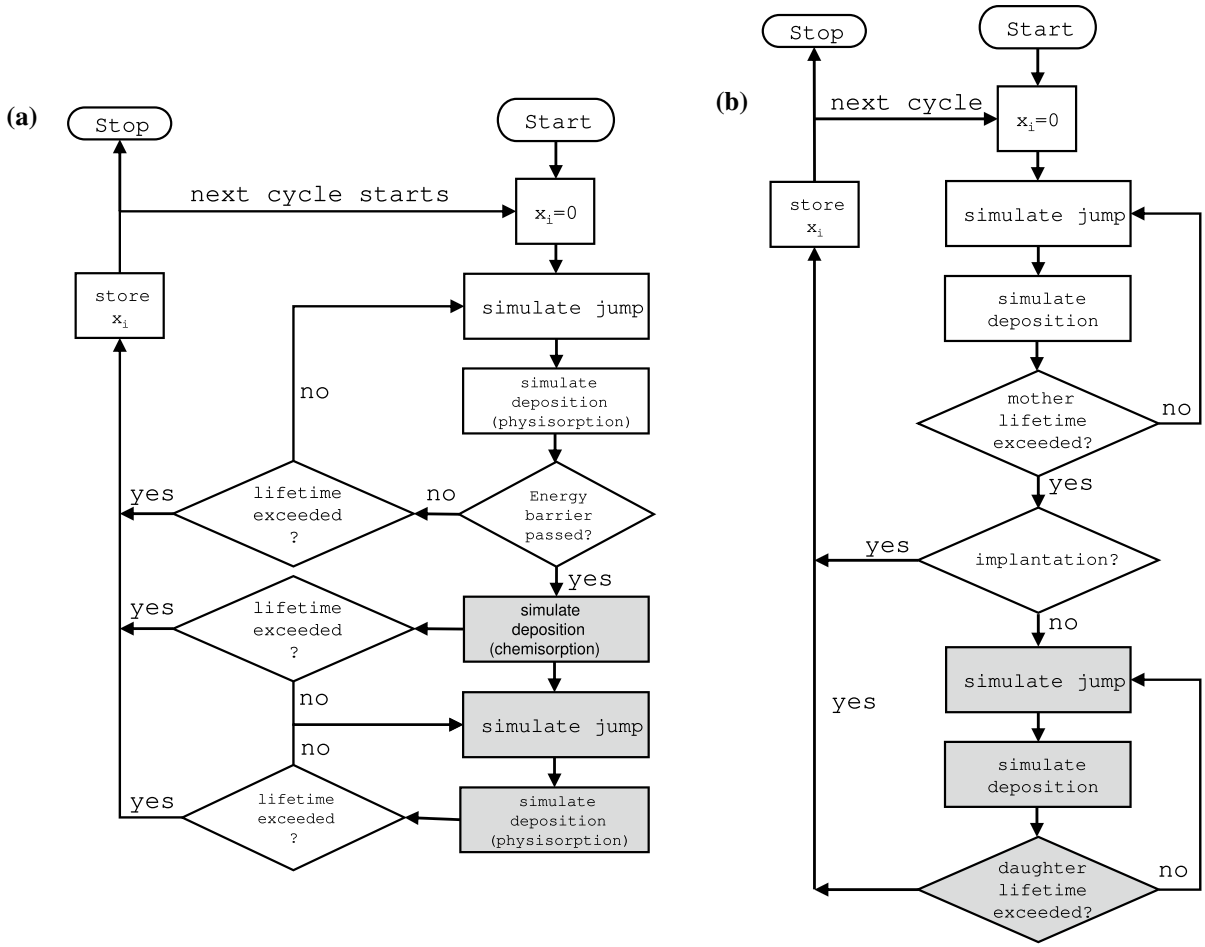

Fig. 2 Flow schemes of the adapted Monte Carlo simulations. **a** with activation energy barrier and second chemical species (grey), **b** with precursor effect, implantation and daughter nuclide (grey). At the start of the simulation, molecular parameters like the masses, densities, adsorption enthalpies, activation energy, lifetime and experimental parameters like temperature, gas mixture, gas flow rate, pressure are set for the first atom. The jump gets simulated by calculating a random jump length and duration η_j and ι_{η_j} between two encounters and adding that value to the current position of the atom. The deposition gets simulated by summing up the deposition time from sequential surface encounters τ_{Ns}. The passing of the energy barrier is tested by the condition *1-random()* < *P*, as described in Eq. (2). If the total time exceeds the individual lifetime, the atom's position gets stored

of an application of the precursor effect for SHE (Fig. 3). Mc as the mother atom could form a distribution within the chromatography column, given fast enough extraction. The Nh atoms then start their journey at the positions, where Mc decayed. The precursor effect extends beyond individual mother and daughter atoms and can be applied to entire decay chains of superheavy elements within a chromatography column. Using these simulations, we can validate the probability of decay positions within the decay chain and estimate the positions of missing events.

The precursor effect was first incorporated into the MCS to simulate the behavior of ^{211}Bi atoms as daughters of the precursor ^{211}Pb. Lead itself forms an exponential distribution in the column, as shown in [33]. In Fig. 2b, a flow scheme of the Monte Carlo simulation including the precursor effect is shown.

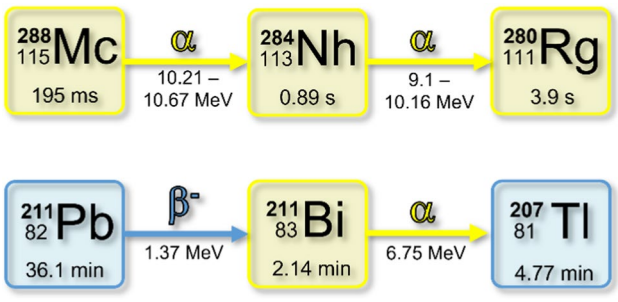

Fig. 3 Examples of decay chains with mother (Mc, Pb) and daughter (Nh, Bi), where the precursor effect has to be considered in the evaluation of chromatography experiments

For two different nuclear species, the simulation also includes two different lifetimes, which are both individually and randomly calculated from the lifetime probability distribution. Furthermore, since mother and daughter atoms can have different masses and densities, an adjustment of the diffusion coefficient after the decay mother → daughter is necessary. Taking the precursor effect into account, the final position of the „mother" atom at the moment of its radioactive decay is the starting position for the „daughter" atom. Thus, the starting position differs: While ^{211}Pb as the mother starts at $x_i = 0$, ^{211}Bi starts at the position where the precursor decayed. The radioactive decay characteristics of the mother also affect the distribution of daughter atoms in the column. For the case of decay by alpha particle emission, the daughter atom can be irreversibly immobilized due to implantation of the recoiling daughter species in the surface. Therefore, an implantation probability was added to the simulation. If the daughter is emitted into the open space of the gas-filled channel, it is likely to travel a significant distance to the next surface contact. In this case, the history of the daughter atom starts with a "long jump" in the gas stream. The atom gets transported downstream and the flight time is calculated. In contrast, low recoil energies from a beta decay result in a recoil range in the gas below 6 µm calculated for typical kinetic energies of below 0.01 keV for a recoil with the mass of 211 u (calculated using SRIM [34]), keeping the atom close to the surface and facilitating immediate re-adsorption. Contrary to the decay of the mother nucleus on the surface by alpha particle emission resulting in the recoil momentum towards gas-filled channel, the history of the daughter atom after the beta-decay could begin with the adsorption step, rather than a "jump" as the first step. Therefore, the random residence time is calculated as the initial step in the process. Especially for non-volatile daughter atoms like ^{211}Bi, the distribution of bismuth would resemble the distribution of its mother lead, because it is almost certain, that the atom will remain adsorbed until its lifetime has elapsed. Since it is not clear, which fraction of atoms adsorb or jump first, both cases have to be considered and discussed. In cases where the precursor is volatile, the mother atom may have already exited the column before decaying into the daughter. The mean adsorption time (Eq. (1)), $\overline{\tau}_a$, for the "mother" and "daughter" nucleus has to be calculated with the adsorption enthalpy values ΔH_{ads}(mother) and ΔH_{ads}(daughter) for mother and daughter species, respectively. In general, both species likely have a different interaction strength, and thus, different enthalpy values should be taken for the residence time calculation.

Results obtained with the extended Monte Carlo simulation code and discussion

Chemical reactions superimposing the mobile adsorption process

The following examples demonstrate the effects of the processes that were explicitly added in the extended MCS code, including a potential transition over an activation barrier to a stronger binding state. Assuming the following experimental observation: A species is relatively volatile at ambient temperature in isothermal experiments, but exhibits lower volatility at elevated temperatures. These observations suggest a conversion of the volatile species into a less-volatile one at temperature, in which the surface reaction is likely. The conventional Monte Carlo simulation fails to account for this behavior, since only one species can be simulated. However, if a strongly bound state can be reached only by passing an activation barrier E_a, higher than the adsorption enthalpy $\Delta H_{ads,1}$, the enhanced simulations can reproduce this behavior. At high temperatures, the volatile species undergoes a reaction with the surface, leading to the formation of a less volatile second species. This second species becomes strongly bound to the surface, causing it to be immobilized even at elevated temperatures. Upon further heating, this second non-volatile species is eventually desorbed. In contrast, at room temperature, the probability of surpassing the activation barrier is low and thus, the species can be desorbed without any chemical interaction with the surface taking place or before diffusing to a strongly binding site. Additionally, it is possible that at high temperature regimes, surface diffusion is fast, transporting the adsorbed species to stronger binding sites, while the desorption process might be faster than the transport on the surface at lower temperature. More information about surface diffusion can be found in [20], which discusses the most recent experiment with element 114. Our extended MCS code is also able to describe the appearance of two deposition peaks at different temperatures in a thermochromatographic setup. In higher temperatures, the probability of overcoming the activation barrier increases, facilitating a strong bond with the surface. However, if some of these atoms get transported to colder regions, the barrier is too high and only $\Delta H_{ads,1}$ contributes to the deposition time.

For these example simulations, a hypothetical species of 200 u atomic weight and with a half-life of 1 h was chosen. The change in mass of the reacted species was neglected, since mainly the difference in the adsorption enthalpy has an influence on the obtained distributions. Helium gas was used at a flow rate of 100 mL/min. A 100-cm long circular quartz column with inner radius of 2 mm was used. In

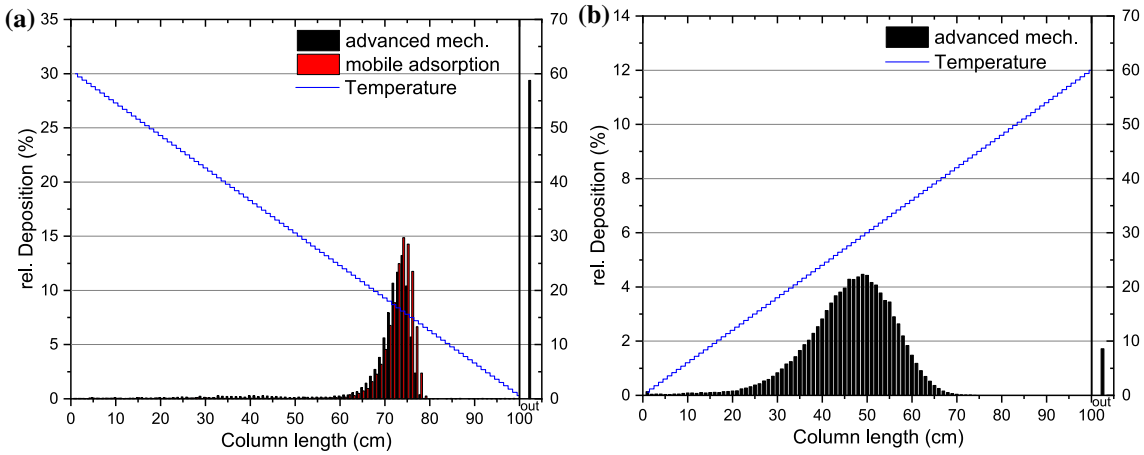

Fig. 4 **a** Comparison of simulated thermochromatography experiments (with negative temperature gradient) using both mobile adsorption and the activated adsorption mechanism. **b** Simulation results of thermochromatography experiments (with positive temperature gradient) utilizing the activated adsorption mechanism. In the mobile adsorption case, 100% deposition occurs within the initial centimeter (not shown). The gas carrying the analyte enters the column from the left. Parameters in kJ/mol: $\Delta H_{ads,1} = 50$; $E_a = 100$; $\Delta H_{ads,2} = 300$

Fig. 4a, the atoms deposit and undergo decay within the same temperature zone. The atoms promptly react in the hot temperature regime, leading to the formation of the less volatile species 2, which then deposits around 160 °C. In the case of the TC with positive gradient (Fig. 4b) the opposite holds true: While the species with the mobile adsorption mechanism deposits immediately in the cold temperature regime (not displayed), the advanced simulation shows the species remaining volatile until it reaches the reaction temperature. Here, the reaction product, which is non-volatile at these temperatures, remains deposited at the reaction site. These examples highlight that relying on a single thermochromatography experiment will lead to erroneous interpretations if chemical reactions, which may occur in some chemical systems, are not considered in the analysis by MCS.

The simulation showcased here is a tool to describe unexplained phenomena and enhances our understanding of how volatile and non-volatile species behave at varying temperatures. By considering the effects of chemical reactions and temperature-dependent interactions with the surface, the simulation offers a deeper understanding of the complex dynamics in thermochromatography experiments.

Precursor effect and implantation probability

Simulations using the extended MCS code were performed for the genetically linked $^{211}Pb \rightarrow {}^{211}Bi$ case using both, the original MCS algorithm [23] and the extended one, which includes the precursor effect. Figure 5 shows the distributions of Bi at the positions of the radioactive decay from the original MCS code and from the extended one. In these simulations, a gas flow rate of 3 L/min of pure Ar was used; circular quartz chromatography columns with an inner of 2 mm and a length of 15 cm were assumed. Standard temperature and pressure (STP) conditions were used.

In the simulations including the precursor effect, two lifetimes, for the mother and the daughter atom respectively, were generated from the individual lifetime probability distribution. The ^{211}Bi daughter atoms originating from the beta-decay of ^{211}Pb can desorb for further travelling in the gas stream unless they become implanted and immobilized.

One can see that the distributions of the daughter atoms including the precursor effect are broader, especially if no implantation takes place. This effect becomes more pronounced for smaller absolute values of $\Delta H_{ads.}$ of the daughter species, as can be seen in Fig. 6, where this value was reduced to − 50 kJ/mol compared to − 100 kJ/mol in Fig. 5. The lower absolute value, corresponding to higher volatility, increases the likelihood of multiple jumps during the lifetime and allows daughter atoms to exit the column after the decay of the mother species. Figure 6 shows a comparison of distributions obtained with different adsorption enthalpies for the mother and daughter nuclei. The mother is non-volatile, while the daughter is volatile.

Without implantation, the volatile daughter atom can exit the column following the decay of the non-volatile mother atoms (Fig. 6a). Figure 6b shows the implantation of the daughter atoms following the precursors decay and the subsequent immobilization of the volatile daughter atoms, which would otherwise exit the column (6a). If the implantation probability is set to 50%, only half of the volatile daughter atoms can travel further down the column. In simulations with the original MCS code, this could lead to incorrect interpretations of experimental results, as the deposition in the column caused by implantation suggests

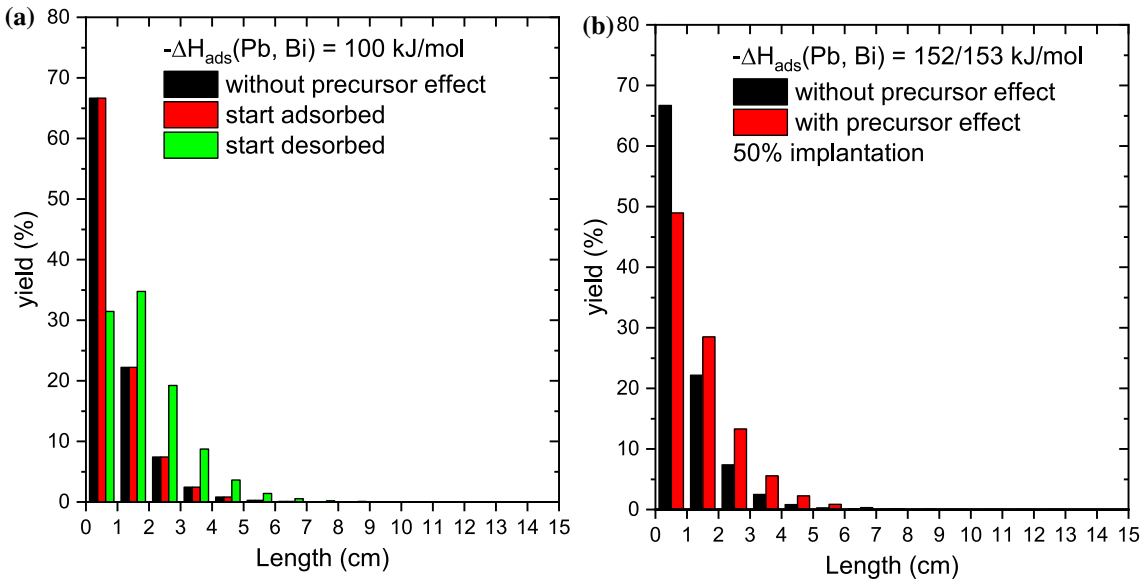

Fig. 5 Results of Monte Carlo simulations of an isothermal gas chromatography experiment with ^{211}Pb, which decays into ^{211}Bi, performed inside of a 15-cm long quartz column with 2 mm inner diameter held at room temperature and using 3 L/min of pure Ar as carrier gas. Results indicating the position where ^{211}Bi atoms decay obtained with the original MCS code (black bars) as well as with the extended MCS code that includes the precursor effect (red bars) are shown. The results of the extended MCS code in 4a) neglects the possibility that progenies of ^{211}Pb might get implanted into the column in the ^{211}Pb β^--decay process—corresponding to all daughter atoms starting adsorbed or desorbed ("in flight"), while 4b) assumes that 50% of the decays lead to implanted and thus immobile progenies. For Pb as well as for Bi atoms, the value of the adsorption enthalpy, ΔH_{ads}, was set to − 100 kJ/mol to demonstrate the peak-broadening for non-volatile species

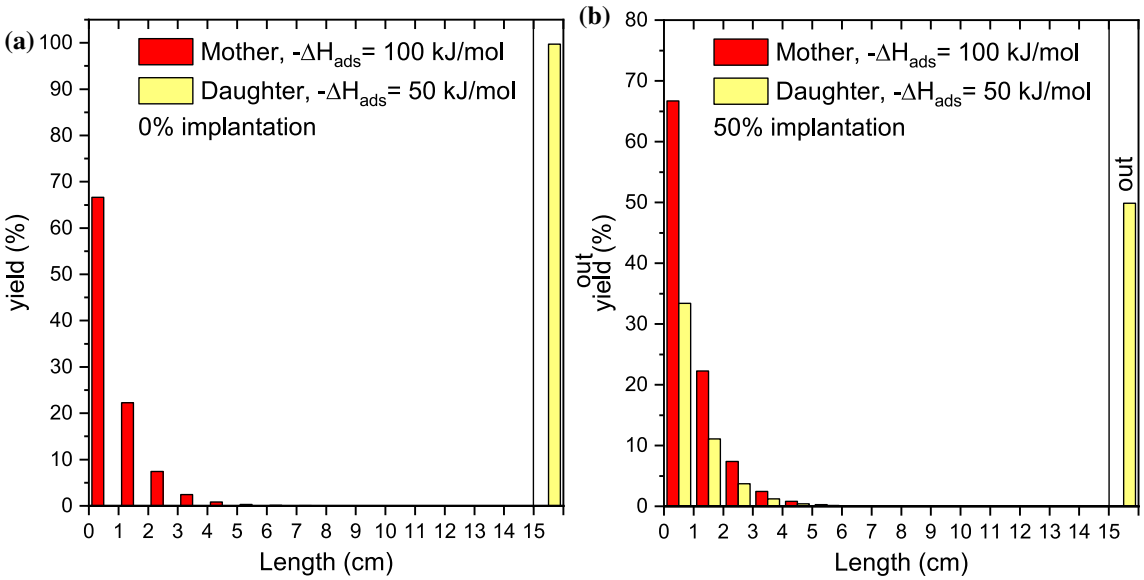

Fig. 6 Comparison of the distribution of decay activity of the non-volatile mother and volatile daughter atoms in the column with 0% and 50% implantation of the daughter with experimental parameters similar to Fig. 5. This figure shows the difference between the mothers and the daughters distribution, simulated with the code that includes the precursor effect

a strongly interacting species. If the direct measurement of the mother atoms decay is not possible, the distribution of the daughter can provide a reasonable estimation for the reactivity of the mother atom. If the detection of the mother atom is not possible, the registered distribution of daughter atoms can reflect the mother distribution,

if the daughter atoms interact strongly with the surface. There would certainly be no exponential distribution of the daughter atoms, if the mother is volatile and only randomly decays in-flight. This effect was used in L. Lens et. al [33] to determine the adsorption enthalpy of Tl by detection of the Hg distribution on the SiO_2 surface, where Hg atoms were partially immobilized on the surface due to implantation after the decay of Tl. If the mother was volatile, while the daughter was non-volatile or reactive, the distribution of both atoms would appear flat. Mother atoms only decay randomly in-flight while passing through the column, and the daughter atom adsorbs at the position where its mother decayed. Implantation or recoiling effects can be neglected due to the short residence time of the mother on the surface. The same holds true, if both species are volatile, as both mother and daughter atoms undergo random decay in the gas stream. If the adsorption enthalpy of the daughter is well known and the experimental data has sufficient statistical significance, it is possible to reconstruct the distribution of the precursor and estimate its adsorption enthalpy.

Outlook and possible applications

With of the MCS including the precursor effect, experiments searching for new decay modes, that are challenging to detect in modern setups could be evaluated. In the long alpha-chain following the ^{288}Mc chain, all species (Nh, Rg, Mt) are rather non-volatile. The characteristics of this long chain are well known [35–37]. But also shorter decay chains were detected, in which the origin of the fission is unclear. A possible electron catch (transition from odd-Z to even-Z elements) in a shorter decay chain of moscovium could end with the fission of copernicium or darmstadtium. If this EC occurs in Mc (presumably non-volatile [38]), it would lead to the more volatile flerovium [15, 20]. If the EC occurs in element 113, nihonium [17, 39, 40], it decays to the more volatile copernicium, element 112 [18, 19]. In contrast to the odd Z elements of the decay chain of moscovium, flerovium and copernicium are more volatile and can be separated from non-volatile elements of the Mc-chain by gas chromatography and detected in a different place than their precursor. Such an experiment has to be evaluated using the new MCS with the precursor effect. If the detection places of the fission fragments are in agreement with the results from the MCS simulation, the electron catch in ^{288}Mc or ^{284}Nh can be proven.

Acknowledgements This work was supported by the German Federal Ministry of Education and Research (BMBF) under contract Nr. 05P21UMFN2.

Data availability The simulation data and code will be made available upon request, provided that such a request is accompanied by a valid and justifiable reason for accessing the data.

Declarations

Conflict of interest The authors declare no competing interest.

References

1. Türler A, Eichler R, Yakushev A (2015) Chemical studies of elements with Z⩾ 104 in gas phase. Nucl Phys A 944:640–689. https://doi.org/10.1016/j.nuclphysa.2015.09.012
2. Schädel M (2006) Chemistry of superheavy elements. Angew Chem Int Ed Engl 45:368–401. https://doi.org/10.1002/anie.200461072
3. Türler A, Pershina V (2013) Advances in the production and chemistry of the heaviest elements. Chem Rev 113:1237–1312. https://doi.org/10.1021/cr3002438
4. Oganessian YT, Utyonkov VK (2015) Super-heavy element research. Rep Prog Phys 78:36301. https://doi.org/10.1088/0034-4885/78/3/036301
5. Hoffman DC, Lee DM (1999) Chemistry of the Heaviest Elements- One Atom at a Time. J Chem Educ 76:331. https://doi.org/10.1021/ed076p331
6. Hübener S, Taut S, Vahle A et al (2001) Physico-chemical characterization of seaborgium as oxide hydroxide. Radiochim Acta 89:737–742. https://doi.org/10.1524/ract.2001.89.11-12.737
7. Eichler R, Brüchle W, Dressler R et al (2000) Chemical characterization of bohrium (element 107). Nature 407:63–65. https://doi.org/10.1038/35024044
8. Chiera NM, Sato TK, Eichler R et al (2021) Chemical characterization of a volatile Dubnium compound, $DbOCl_3$. Angew Chem Int Ed 60:17871–17874. https://doi.org/10.1002/anie.202102808
9. Türler A, Brüchle W, Dressler R et al (1999) First measurement of a thermochemical property of a seaborgium compound. Angew Chem Int Ed 38:2212–2213. https://doi.org/10.1002/(SICI)1521-3773(19990802)38:15%3c2212:AID-ANIE2212%3e3.0.CO;2-6
10. Gäggeler HW, Jost DT, Baltensperger U et al (1991) OLGA II, an on-line gas chemistry apparatus for applications in heavy element research. Nucl Instrum Methods Phys Res, Sect A 309:201–208. https://doi.org/10.1016/0168-9002(91)90103-W
11. Eichler R, Eichler B, Gäggeler HW et al (1999) The gas phase oxide and oxyhydroxide chemistry of trace amounts of Rhenium. Radiochim Acta 87:151–160. https://doi.org/10.1524/ract.1999.87.34.151
12. Düllmann CE, Eichler B, Eichler R et al (2002) IVO, a device for In situ volatilization and on-line detection of products from heavy ion reactions. Nucl Instrum Methods Phys Res, Sect A 479:631–639. https://doi.org/10.1016/S0168-9002(01)00898-1

13. Kirbach U, Folden C III, Ginter T et al (2002) The cryo-thermochromatographic separator (CTS). Nucl Instrum Methods Phys Res Sect A 484:587–594. https://doi.org/10.1016/S0168-9002(01)01990-8
14. Düllmann CE, Dressler R, Eichler B et al (2003) First chemical investigation of hassium (Hs, Z=108). Czech J Phys 53:A291–A298. https://doi.org/10.1007/s10582-003-0037-4
15. Yakushev A, Eichler R (2016) Gas-phase chemistry of element 114, flerovium. EPJ Web Conf 131:7003. https://doi.org/10.1051/epjconf/201613107003
16. Eichler R, Aksenov NV, Albin YV et al (2010) Indication for a volatile element 114. Radiochim Acta. https://doi.org/10.1524/ract.2010.1705
17. Yakushev A, Lens L, Düllmann CE et al (2021) First study on nihonium (Nh, Element 113) chemistry at TASCA. Front Chem 9:753738. https://doi.org/10.3389/fchem.2021.753738
18. Eichler R, Aksenov NV, Belozerov AV et al (2007) Chemical characterization of element 112. Nature 447:72–75. https://doi.org/10.1038/nature05761
19. Eichler R, Aksenov NV, Belozerov AV et al (2008) Thermochemical and physical properties of element 112. Angew Chem Int Ed Engl 47:3262–3266. https://doi.org/10.1002/anie.200705019
20. Yakushev A, Lens L, Düllmann CE et al (2022) On the adsorption and reactivity of element 114, flerovium. Front Chem 10:976635. https://doi.org/10.3389/fchem.2022.976635
21. Guillaumont R, Adloff JP, Peneloux A (1989) Kinetic and thermodynamic aspects of tracer-scale and single atom chemistry. Radiochim Acta 46:169–176. https://doi.org/10.1524/ract.1989.46.4.169
22. Eichler B, Zvara I (1982) Evaluation of the enthalpy of adsorption from thermochromatographical data. Radiochim Acta 30:233–238. https://doi.org/10.1524/ract.1982.30.4.233
23. Zvára I (1985) Simulation of thermochromatographic processes by the Monte Carlo method. Radiochim Acta 38:95–102. https://doi.org/10.1524/ract.1985.38.2.95
24. Schädel M, Shaughnessy D (eds) (2014) The chemistry of superheavy elements, 2nd edn. Springer, Berlin
25. Pershina V (2019) Relativity in the electronic structure of the heaviest elements and its influence on periodicities in properties. Radiochim Acta 107:833–863. https://doi.org/10.1515/ract-2018-3098
26. Zvára I (2008) The inorganic radiochemistry of heavy elements: methods for studying gaseous compounds. Springer, New York
27. Dvorak J, Brüchle W, Chelnokov M et al (2006) Doubly magic nucleus (108)(270)Hs162. Phys Rev Lett 97:242501. https://doi.org/10.1103/PhysRevLett.97.242501
28. Serov A, Aksenov NV, Bozhikov GA et al (2011) Adsorption interaction of astatine species with quartz and gold surfaces. Radiochim Acta 99:593–600. https://doi.org/10.1524/ract.2011.1850
29. Eichler B (1996) The behaviour of chlorides of radionuclides in gas adsorption chromatographic processes with superimposed chemical reactions. Radiochim Acta 72:19–26
30. Even J, Yakushev A, Düllmann CE et al (2014) Nuclear chemistry. Synthesis and detection of a seaborgium carbonyl complex. Science 345:1491–1493. https://doi.org/10.1126/science.1255720
31. Lennard-Jones JE (1932) Processes of adsorption and diffusion on solid surfaces. Trans Faraday Soc 28:333. https://doi.org/10.1039/tf9322800333
32. Brass SG, Ehrlich G (1986) Activated chemisorption: Internal degrees of freedom and measured activation energies. Phys Rev Lett 57:2532–2535. https://doi.org/10.1103/PhysRevLett.57.2532
33. Lens L, Yakushev A, Düllmann CE et al (2018) Online chemical adsorption studies of Hg, Tl, and Pb on SiO 2 and Au surfaces in preparation for chemical investigations on Cn, Nh, and Fl at TASCA. Radiochim Acta 106:949–962. https://doi.org/10.1515/ract-2017-2914
34. Ziegler JF, Biersack J, Ziegler MD (2015) SRIM - the stopping and range of ions in matter. SRIM, Chester, Maryland
35. Forsberg U, Rudolph D, Andersson L-L et al (2016) Recoil-α-fission and recoil-α–α-fission events observed in the reaction 48Ca + 243Am. Nucl Phys A 953:117–138. https://doi.org/10.1016/j.nuclphysa.2016.04.025
36. Oganessian YT, Utyonkov VK, Kovrizhnykh ND et al (2022) First experiment at the Super Heavy Element Factory: high cross section of Mc288 in the Am 243+Ca48 reaction and identification of the new isotope Lr264. Phys Rev C. https://doi.org/10.1103/PhysRevC.106.L031301
37. Rudolph D, Sarmiento L, Forsberg U (ed) (2015) Nuclear structure notes on element 115 decay chains. In: AIP conference proceedings. AIP Publishing LLC
38. Pershina V, Iliaš M, Yakushev A (2021) Reactivity of the superheavy element 115, Mc, and its lighter homologue, Bi, with respect to gold and hydroxylated quartz surfaces from periodic relativistic DFT calculations: a comparison with element 113, Nh. Inorg Chem 60:9796–9804. https://doi.org/10.1021/acs.inorgchem.1c01076
39. Aksenov NV, Steinegger P, Abdullin FS et al (2017) On the volatility of nihonium (Nh, Z = 113). Eur Phys J A. https://doi.org/10.1140/epja/i2017-12348-8
40. Dmitriev SN, Aksenov NV, Albin YV et al (2014) Pioneering experiments on the chemical properties of element 113. Mendeleev Commun 24:253–256. https://doi.org/10.1016/j.mencom.2014.09.001